Photoinduced instability of the magnetic structure of hexagonal $ScMnO_3$

M. Fiebig,[1,*] D. Fröhlich,[1] Th. Lottermoser,[1] and R. V. Pisarev[2]
[1]*Institut für Physik, Universität Dortmund, D-44221 Dortmund, Germany*
[2]*Ioffe Physical Technical Institute of the Russian Academy of Sciences, St. Petersburg 194021, Russia*
(Received 25 February 2002; published 6 June 2002)

A modification of the magnetic structure was observed in hexagonal antiferromagnetic $ScMnO_3$ upon transmission of an intense near-infrared light pulse. Photomagnetic effects lead to a rotation of the magnetic moments inside the basal plane of the Mn^{3+} lattice for which the presence of a weak ferromagnetic moment along the hexagonal axis of our single crystals could not be confirmed. Further, movement of antiferromagnetic domain walls and the creation of new walls were observed. The effects exhibit a distinct dependence on the linear polarization of the incident light while circular photomagnetic effects were not detected. This is explained by a photoinduced modification of the magnetic anisotropy.

DOI: 10.1103/PhysRevB.65.224421 PACS number(s): 75.60.Ch, 42.65.Sf, 75.25.+z, 42.65.Ky

The hexagonal manganites $R\mathrm{MnO_3}$ (R=Sc, Y, In, Ho–Lu) are an interesting group of compounds due to an unusual combination of electric and magnetic properties. The compounds are ferroelectric[1] and show additional magnetic ordering of the Mn^{3+} and, in some cases, the R^{3+} sublattices all of which are geometrically frustrated.[2,3] The multifold ordering and the high degree of correlation between the different sublattices lead to rich phase diagrams with a possibility for hidden phase transitions[4] and a general instability of the magnetic structure. A coexistence of different magnetic phases,[5,6] orientational magnetic phase transitions,[4,6] and the possibility to control the lateral dimension of antiferromagnetic domains within a range spanning two orders of magnitude[7] manifest the magnetic instability. Due to the competition between different magnetic phases, the magnetic structure is quite sensitive to a variation of external parameters. Magnetic phase control is exerted by an application of moderate magnetic fields,[4,8] whereas the topography of the antiferromagnetic domain structure can be controlled by proper temperature annealing *above* the ordering temperature.[7] Due to a correlation between the long-range electric and magnetic ordering, the magnetic domain structure can also be influenced by the application of electric fields,[9] which is an interesting property for technical applications.[10,11] With its high sensitivity to static electric and magnetic fields, a modification of the magnetic order of this highly correlated system may also be expected from the dynamic electromagnetic fields of an incident light wave. However, whereas such a coupling is well known from the orthorhombic ''colossal magnetoresistive'' manganites, it has not yet been observed for the hexagonal $R\mathrm{MnO_3}$ system.

In this paper, we investigate the influence of an intense light field on the magnetic structure of $ScMnO_3$. A pronounced modification of the antiferromagnetic order with an unusual dependence on the polarization of the incident light wave is observed. This is explained by photomagnetic coupling in combination with a small magnetic anisotropy in the easy plane of the compound.

All the hexagonal compounds from the $R\mathrm{MnO_3}$ series are ferroelectric at room temperature, the space group being $P6_3cm$.[1] At 70–130 K magnetic ordering of the Mn^{3+} sublattice occurs in all compounds but $InMnO_3$. The Mn^{3+} lattice consists of basal xy planes in which an antiferromagnetic 120° arrangement of Mn^{3+} spins breaks the geometric frustration of the hexagonal lattice.[2,3] The Mn^{3+} planes are stacked along the hexagonal z axis with a weak antiferromagnetic (α type[2]) coupling between neighboring planes[12] as shown in the inset of Fig. 1. In spite of strong antiferromagnetic coupling within the basal plane the in-plane anisotropy is small and unstable against a variation of temperature or application of a magnetic field. Therefore, the angle φ_{spin} included between the Mn^{3+} spin and the x axis (the axis

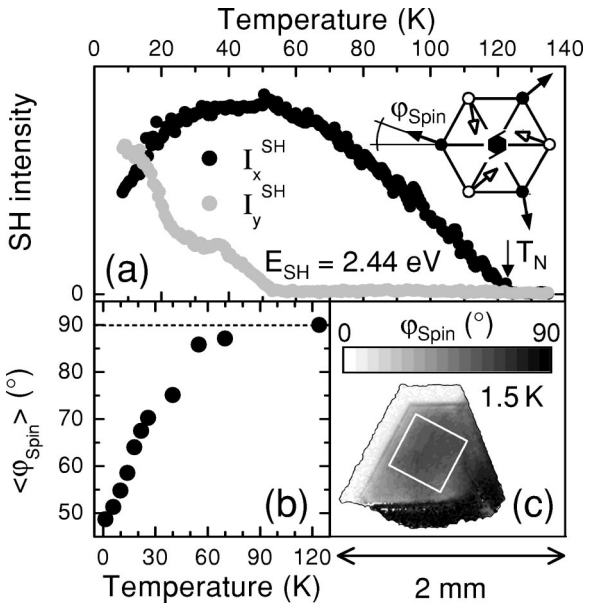

FIG. 1. Instability of the magnetic structure of hexagonal $ScMnO_3$. (a) SH intensity at 2.44 eV as function of temperature. I_x^{SH} and I_y^{SH} denote the x and y polarized component of the SH intensity emitted from a confined region of the sample in (c). The inset shows the antiferromagnetic structure in the basal plane with open (closed) circles denoting Mn spins at $z=0$ ($z=c/2$) in the unit cell. (b) Averaged orientation of the Mn spin in the unit cell of the sample in (c) with φ_{spin} as defined in (a). (c) Spatial distribution of the local value of φ_{spin} at 1.5 K. Note that values $0°\leqslant\varphi_{\mathrm{spin}}\leqslant 90°$ contribute to the average value $\langle\varphi_{\mathrm{spin}}\rangle=49°$ in (b). The white line in panel (c) marks the integration area for Fig. 3.

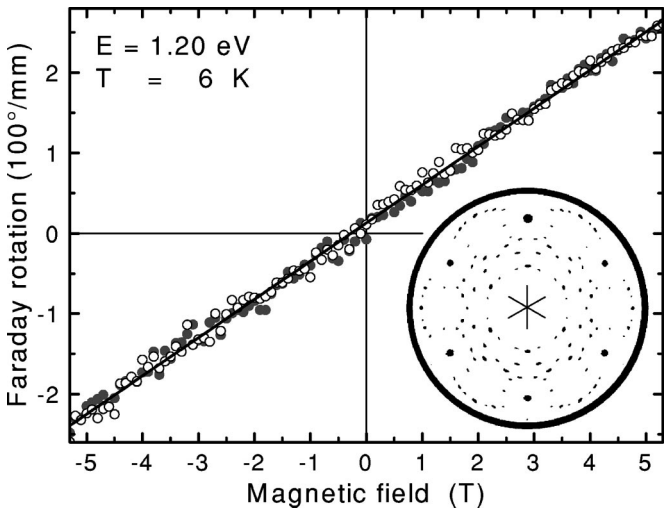

FIG. 2. Faraday rotation of the $ScMnO_3$ sample shown in Fig. 1(c) as function of a static magnetic field applied along the *z* axis. Closed and open circles show the rotation measured in field increasing and decreasing runs, respectively. The inset shows an x-ray transmission pattern of the sample with the asterisk indicating the directions of the three *x* axes.

perpendicular to the glide plane *c*)[13] can assume arbitrary values in the *xy* plane.

Among the hexagonal manganites, the properties of $InMnO_3$ and $ScMnO_3$ stand forth. $InMnO_3$ does not show long-range magnetic ordering due to the large distance between neighboring Mn^{3+} planes along *z*. $ScMnO_3$, on the other hand, possesses the smallest distance among the hexagonal $RMnO_3$ compounds.[14] The Néel temperature of $ScMnO_3$ is 50–90% higher than that of the other $RMnO_3$ compounds. Further, measurements of the temperature dependence of the magnetic susceptibility and the specific heat of $ScMnO_3$ deviate from those of other $RMnO_3$ compounds in that a distinct sensitivity of the Mn^{3+} sublattice to an externally applied magnetic field with large entropy contributions from the magnetic subsystem below T_N is observed.[8,15,16] These results suggest that $ScMnO_3$ plays a prominent role as end compound of the $RMnO_3$ series (opposite of $InMnO_3$) in which many of the effects guiding the magnetic properties of this series are enhanced. Moreover, the case of $ScMnO_3$ polarizes the ongoing discussion about the magnetic structure of hexagonal $RMnO_3$, because for this system many different types of crystallographic and magnetic ordering were reported which are not compatible with each other. In particular, several authors report the observation of spin canting or a weak ferromagnetic moment[17–19] which is incompatible with antiferromagnetic coupling between the basal Mn planes. Due to the key role $ScMnO_3$ apparently assumes in the series of hexagonal manganites we restrict ourselves to the investigation of this compound in the following.

In the experiment polished flux-grown (0001) single-crystal platelets of $ScMnO_3$ with thicknesses of about 0.1 mm and lateral dimensions of 1–3 mm were used.[20] The samples were x rayed prior to the experiment. With x rays perpendicular to the sample surface one obtains the diffraction pattern shown as inset in Fig. 2. It displays a sixfold symmetry with well-focused reflexes, which points to a well oriented ($<0.1°$) sample free of stacking faults, twinning, and other gross growth errors. Light pulses at $\hbar\omega=1.22$ eV from an optical parametric oscillator (3 mJ, 3 ns, repetition rate 10−40 Hz) were used to photoexcite the samples which are transparent below 1.34 eV. Second harmonic generation (SHG) at $2\hbar\omega=2.44$ eV allows us to monitor the effect of the excitation on the magnetic structure of the sample.[5] Wave plates and optical and polarizing filters were used to set the polarization of the incoming light, separate the SH light and the transmitted fundamental light behind the sample, and analyze the polarization of the SH signal. A telephoto lens with a resolution of 10 μm was used to project the signal light onto a cooled CCD camera.[21] In those cases where a magnetic field was applied to the samples, the resulting Faraday rotation was determined directly from the polarization of the light transmitted through the samples, which was detected with a photodiode.

The investigation of noncentrosymmetric magnetocrystalline structures by SHG is based on the relation between the induced nonlinear polarization $P_i(2\omega)$ and the electric field components $E_j(\omega)$ and $E_k(\omega)$ of the fundamental light

$$P_i(2\omega)=\epsilon_0\chi_{ijk}E_j(\omega)E_k(\omega). \tag{1}$$

The tensor components χ_{ijk} are induced by crystallographic or magnetic ordering in the sample. They are unarbitrarily related to the corresponding space symmetry and can be identified experimentally by measuring the intensity of the SH signal $I_i^{\mathrm{SH}}(2\omega)\propto|P_i(2\omega)|^2$ for various directions and polarizations of the incident and emitted light. Knowing a selected set of tensor elements χ_{ijk} is often sufficient to draw conclusions on the magnetic structure of a compound. In the hexagonal manganites, most convenient access to the magnetic structure is achieved with light incident along the hexagonal *z* axis, since in this configuration all the tensor components coupling to the crystallographic structure do not contribute to SHG. The only independent components for $k\|z$ are χ_{xxx} and χ_{yyy} for antiferromagnetic coupling (α type) between neighboring Mn^{3+} planes. Note that in the case of ferromagnetic coupling (β type) SH contributions are not allowed so that any observation of a SH signal for $k\|z$ immediately rules out the possibility for ferromagnetic interplane coupling.[5] According to Refs. 6 and 9, the polarization of the emitted SH wave is directly correlated to the orientation of the Mn^{3+} spins in the basal plane and thus, to the value of φ_{spin} as shown in the inset of Fig. 1(a). One finds

$$\tan^2\varphi_{\mathrm{spin}}=\xi(\omega)I_x^{\mathrm{SH}}/I_y^{\mathrm{SH}} \tag{2}$$

with $I_x^{\mathrm{SH}}\propto|\chi_{xxx}|^2$ and $I_y^{\mathrm{SH}}\propto|\chi_{yyy}|^2$ as *x* and *y* polarized contribution to the total SH intensity after excitation with light polarized along either the *x* or the *y* axes.[6] The factor $\xi(\omega)$ depends on the photon energy and compensates the difference in magnitude of χ_{xxx} and χ_{yyy} at the end values $\varphi_{\mathrm{spin}}=0°$ and 90°.

Figure 1 shows the intensity of the SH signal emitted from a $ScMnO_3$ sample as function of temperature and polarization, and the orientation of the Mn^{3+} spins in the basal plane derived from this measurement by use of Eq. (2). The SH signal in Fig. 1(a) was gained with fundamental *y* polarized light incident along the hexagonal *z* axis of the crystal.

The two graphs correspond to the *x* and *y* components of the emitted SH intensity. The data points are gained by integrating the signal from a fixed region on the homogeneously illuminated sample. In the temperature range $T_N > T > 55$ K, the SH light is *x* polarized so that I_y^{SH} vanishes. Below 55 K, however, the polarization of the SH light deviates from the *x* axis. I_y^{SH} starts to increase while I_x^{SH} is more and more attenuated until at 15 K the two contributions are of approximately equal intensity.

Using Eq. (2) the averaged value $\langle \varphi_{spin} \rangle$ was determined as function of temperature in Fig. 1(b). Contrary to Fig. 1(a), the SH signal was now integrated across the complete area of the sample platelet so that $\langle \varphi_{spin} \rangle$ denotes the average spin angle of the sample. In agreement with Fig. 1(a), the $ScMnO_3$ sample shows a gradual decrease of $\langle \varphi_{spin} \rangle$ from 90° at 70 K to 49° at 1.5 K. The spin rotation does not proceed at a constant rate, so that a kink is observed in the plots in Figs. 1(a) and 1(b) when the rotation stagnates near 40 K. The slow unsteady rotation which stops at some intermediate angle at low temperature points to a very small anisotropy in the basal plane. This is confirmed by the spatially resolved image of the spin angle in Fig. 1(c) which reveals that the average value of $\langle \varphi_{spin} \rangle = 49°$ at 1.5 K in Fig. 1(b) is in fact made up from local variations of φ_{spin} between 0° and 90°.

The small easy-plane anisotropy distinguishes $ScMnO_3$ clearly from hexagonal $RMnO_3$ compounds where due to a large anisotropy a spin reorientation below T_N is not observed. Even in those compounds which exhibit magnetic phase transitions below T_N, these transitions are usually determined by intrinsic changes of parameters, which, e.g., in the case of $HoMnO_3$ leads to a magnetic reorientation occuring across a very narrow temperature range with an abrupt switching of φ_{spin} between the two end values 0° and 90°. In $ScMnO_3$, however, the observed phase transition is dominated by extrinsic effects such as small variations of the stoichiometry during sample growth or strain induced by the preparation process. Therefore, it is the only compound in which an arbitrary orientation of the Mn^{3+} spins in the easy plane is observed in an extended temperature interval. The magnetic instability of the hexagonal $RMnO_3$ system in the basal plane is thus most pronounced in $ScMnO_3$ which makes it particularly suitable for an investigation of light-induced effects with φ_{spin} playing the role as sensor for the perturbation.

Concerning the magnetic stability of the $ScMnO_3$ system perpendicular to the basal plane, a weak ferromagnetic component along the hexagonal axis was reported for polycrystalline $ScMnO_3$ samples by various authors.[17–19] However, weak ferromagnetism is in disagreement with both Figs. 1 and 2. The selection rules for SHG which follow from the polarization dependence of the signal in Fig. 1 inevitably point to the spin structure shown as an inset in the figure. The symmetry of this structure is given by the space group $P\underline{6}_3cm, P\underline{6}_3$, or $P\underline{6}_3\underline{c}m$ depending on the value of φ_{spin} being 0°, between 0° and 90°, or 90°, respectively. In none of these space groups a weak ferromagnetic component perpendicular to the basal plane is allowed. On the other hand, for those magnetic space groups which allow the presence of weak ferromagnetism, a SH signal for light incident along the hexagonal axis is strictly forbidden.

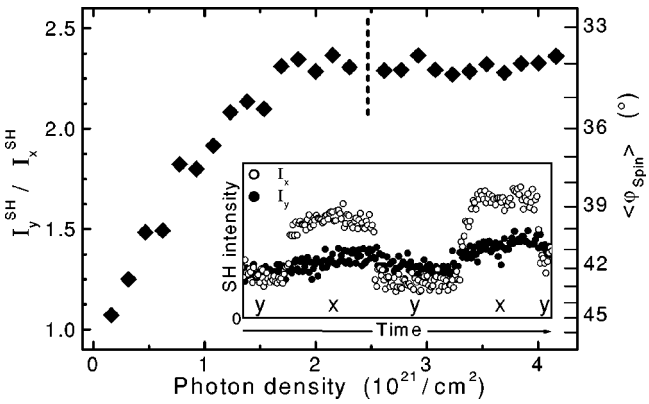

FIG. 3. Ratio I_y^{SH}/I_x^{SH} of the *y* and *x* polarized contributions to the SH intensity at 6 K as function of the density *n* of incident *y* polarized photons with 1.22 eV photon energy and flux $F = 3.6 \times 10^{17}$ cm^{-2} s^{-1} ($F = dn/dt$). The right axis shows the associated value of the average spin angle $\langle \varphi_{spin} \rangle$. The SH light was emitted from the framed region of the $ScMnO_3$ sample in Fig. 1(c). At the dashed line, the photon flux was blocked for several minutes. The inset shows the temporal evolution of I_y^{SH} and I_x^{SH} over a time scale of more than 1 h for repeated switching of the polarization of the incident light between *x* and *y* as indicated in the figure.

Figure 2 shows the Faraday rotation of the sample from Fig. 1(c) as function of a static magnetic field applied along the hexagonal axis. Faraday rotation couples linearly to an applied magnetic field or an intrinsic magnetization and is therefore a suitable sensor for the detection of a spontaneous or imposed magnetic order.[4] In Fig. 2 the rotation increases linearly with the applied field, and in field decreasing runs, upon field reversal, or after excitation with a strong laser pulse a hysteresis as, e.g., in Ref. 19 or other deviations from the linear dependence in Fig. 2 are not observed. The presence of a weak ferromagnetic magnetization along the *z* axis in our single-crystal samples can therefore be excluded.

Figure 3 shows the ratio I_y^{SH}/I_x^{SH} for the $ScMnO_3$ sample in Fig. 1(c) for a 600 μm wide region in the center of the sample. The ratio is shown as function of the photon density *n* which is defined by the number of photons irradiated onto a unit area of the homogeneously illuminated sample. The time derivative of *n* leads to the photon flux *F* of the incident laser light. The initial state for the experiment was prepared by annealing the sample by illumination with *x* polarized light at 1.22 eV. The value $n = 0$ is defined by the moment when the polarization of the incident light was switched by 90° from *x* to *y*. Although a change of polarization of the fundamental wave does not change polarization and intensity of the SH wave for constant φ_{spin}, a continuous increase of I_y^{SH}/I_x^{SH} is observed. At $n_0 = 2 \times 10^{21}$ cm^{-2}, the ratio saturates at 235% of its initial value. This corresponds to a change of $\langle \varphi_{spin} \rangle$ in the observed region from $\langle \varphi_{spin}^{max} \rangle = 45°$ at $n = 0$ to $\langle \varphi_{spin}^{min} \rangle = 34°$ at $n = n_0$. The inset of Fig. 3 shows I_y^{SH} and I_x^{SH}, that is, the raw data for the calculation of $\langle \varphi_{spin} \rangle$, monitored over a time interval of more than 1 h. Repeated

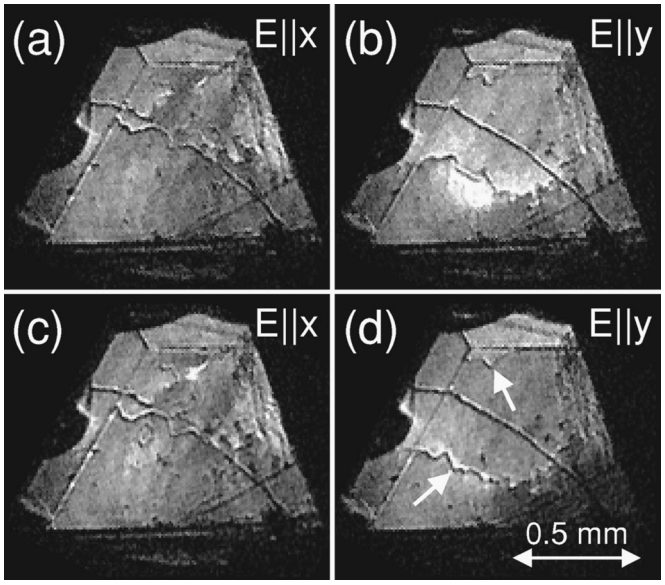

FIG. 4. Antiferromagnetic domain structure of a $ScMnO_3$ sample at 1.5 K upon illumination with linearly polarized light of flux $F=3.6\times10^{17}$ cm^{-2} s^{-1} at 1.22 eV. The domain structure is visualized by the generated SH light with narrow dark lines corresponding to the walls between neighboring domains. Images (a)–(d) were exposed in this sequence after being subjected to a photon density $n>2\times10^{21}$ cm^2 prior to each exposure. The polarization of the incident fundamental light is denoted by *E*. The polarization of the SH light passing the analyzer included 30° with the *x* axis in order to achieve a homogeneous distribution of the brightness of the sample for all values of φ_{spin}.

switching of the polarization of the incident light between *x* and *y* leads to a repeated drastic change of the SH intensities which corroborates that the observed switching of the Mn^{3+} spins is both reversible and reproducible. Moreover, it can be excluded that this decrease is due to a laser-induced increase of temperature in the sample. An increase of temperature can only account for an increase of $\langle\varphi_{\mathrm{spin}}\rangle$.[6] Further, $I_y^{\mathrm{SH}}/I_x^{\mathrm{SH}}$ in Fig. 3 did not change when the laser was blocked for several minutes.

The influence of the light field on the antiferromagnetic domain structure is shown in Fig. 4. In the figure, the spatially resolved SH signal for a $ScMnO_3$ sample is shown for fundamental light polarized along one of the principal axes. Panels (a)–(d) correspond to the temporal sequence of the images. From the emitted SH light the component polarized under 30° to the *x* axis was selected by the analyzer in order to achieve a homogeneous distribution of sample brightness for all values of φ_{spin}. Before recording each image, the sample was exposed to light with a polarization *E* as given in Fig. 4 until the ratio $I_y^{\mathrm{SH}}/I_x^{\mathrm{SH}}$ did not change any further. Each image exhibits narrow dark lines which correspond to the walls between neighboring antiferromagnetic domains. The walls are visible due to an interference effect based on the phase difference in the SH light fields from neighboring domains. Two different types of domain walls can be distinguished. The straight walls separate the phase with $\varphi_{\mathrm{spin}}=0°$ from the phase with $\varphi_{\mathrm{spin}}>0°$. The curved irregular walls separate opposite 180° domains of one magnetic phase. While the position of the straight walls is insensitive to the polarization of the incident laser light, curved walls are moved, removed, or newly created whenever the polarization of the incident light is exchanged between *x* and *y*. There is a clear correlation between the polarization of the incident light and the resulting domain structure since for either polarization a characteristic distribution of domains is reproduced with only small alterations even after repeated switching of the polarization between *x* and *y*. For example, the two domain walls marked by an arrow in Fig. 4(d) are created by the irradiation of *y* polarized incident light. They vanish when the polarization is changed to *x*, and they reappear when it is reverted to *y*.

If circularly polarized light is used for the excitation of the sample, an intermediate spin angle between $\langle\varphi_{\mathrm{spin}}^{\mathrm{max}}\rangle$ and $\langle\varphi_{\mathrm{spin}}^{\mathrm{min}}\rangle$ is assumed by the sample. This angle as well as the antiferromagnetic domain structure appears to be independent of the circular polarization being σ_+ or σ_-.

Photomagnetic effects, that is, photoinduced changes of the magnetic properties of materials have already been studied in a wide range of materials.[22] Common origins for a photoinduced change of the magnetization include transfer of the magnetic moment of the photon spin to the material, trapping of photoexcited carriers into a ''ferron'' state which can modify the exchange interaction locally,[22,23] the formation of Frenkel excitons which modify the magnetic exchange and anisotropy,[22] and the reduction of symmetry by the plane of polarization of the incident light which leads to contributions to the total magnetization.[24] Apart from these single-electron effects, photoinduced insulator-metal transitions may occur due to a shift of the balance between charge-localizing and charge-delocalizing effects in many-electron systems such as the colossal magnetoresistive manganites.[25,26] Even if the magnetic order of a compound is not changed by the irradiated light, photomagnetic effects can lead to a change of the magnetic domain structure due to the formation of potential wells or humps near photogenerated impurities,[22] due to a *local* change of the magnetic order,[23] or due to the total photoinduced magnetization of the sample which shifts the balance between different domains.[27]

In the present case, photomagnetic coupling leads to a change of the antiferromagnetic order in the form of spin rotation and to a change of the antiferromagnetic domain structure. Most remarkably, the photomagnetic effects from circularly polarized light are not larger than those from linearly polarized light, thus reversing the situation which is found in most compounds. In fact, there is no evidence at all for ''true'' circular photomagnetic effects since all the observed effects can be understood as a combination of the linear photomagnetic effects from *x* and *y* polarized light.

The unusual situation can be understood by recalling the different mechanisms for the coupling of circularly and linearly polarized light to the magnetic order. Circularly polarized light can act as a magnetization due to its spin $S_z=\pm1$ and primarily modifies the exchange interaction of a system. In general, these effects are much larger than those exerted by linearly polarized or even unpolarized light which mainly affects the magnetic anisotropy via the reduction of symmetry by the plane of polarization or the direction of the

wave vector.[22] However, $ScMnO_3$ is a system with a strong antiferromagnetic exchange ($\sim$100 T), but a very small anisotropy in the basal plane.[4] Therefore, a photoinduced change of the anisotropy constants by linearly polarized light is expected to have the larger effect in this system in agreement with our observations. Moreover, the enhancement of the linear photomagnetic effect is expected to be confined to the basal plane, since in the relation

$$A(\theta,\phi)=K_1\cos^2\theta+K_2\cos 6\phi \tag{3}$$

describing the anisotropy in hexagonal crystals (with θ and ϕ as spherical coordinates), one usually finds $K_2 \ll K_1$ for the anisotropy constants. Confinement to the basal plane is also in agreement with our observations. Among the possible microscopic origins for the change of anisotropy, the photogeneration of Frenkel excitons as excited states of the partially filled $Mn^{3+}(3d)$ shell may be the most likely one. The creation of the excitons, can lead to very long-lived or even stable states.[28] This can change the magnetic anisotropy to an extent that a variation of the magnetic order, as, e.g., observed in the case of $EuCrO_3$, occurs.[29]

The characteristic dependence of the antiferromagnetic domain structure on the polarization of the incident light can be due to both indirect and direct photomagnetic mechanisms. In the first case, the observed movement, removal, and creation of antiferromagnetic domain walls may be a consequence of the photoinduced variation of φ_{spin} with the polarization. Previous measurements on the $RMnO_3$ system showed that the observed structure and lateral dimension of domains for $P\underline{6}_3$ symmetry is very sensitive to the difference in magnitude between the x and y components of the Mn^{3+} spin[30] which is directly related to φ_{spin}. The correlation between φ_{spin} and the domain structure is further corroborated by the observation that for $n<n_0$ the domain structure is continuously changing along with the rotation of φ_{spin} whereas both φ_{spin} and the observed domain structure do not change any further once the photon density has exceeded n_0.

On the other hand, the electromagnetic field of the incident light wave can directly couple to the long-range magnetic order of the crystal. Evidence for a considerable influence even of small magnetic fields on the magnetic susceptibility of $ScMnO_3$, and thus the domain structure of the crystal, was reported in Ref. 8. The light field may induce a change of the magnetic moments of the ions, thus leading to a magnetization in the material. Since antiferromagnetic domain walls can be regarded as magnetized perturbations the force exerted by the photoinduced magnetization may move them. Pinning effects which locate and hold the antiferromagnetic walls in their position may be attenuated by the polarized light wave in a way which leads to a relocation of the walls and ties them to other pinning centers which are enhanced by the incident light.

In summary, a photomagnetic instability of the antiferromagnetic structure was observed in hexagonal $ScMnO_3$. It originates in a modification of the magnetic anisotropy by the linearly polarized incident light and leads to a rotation in the Mn^{3+} spins in the basal plane with zero magnetic moment along the hexagonal axis. The photomagnetic instability further leads to a movement of antiferromagnetic domain walls or the creation of new walls with a distinct dependence on the polarization of the incident light wave. Various direct and indirect photomagnetic mechanisms contributing to these effects were discussed.

The authors thank K. Kohn for samples and the Deutsche Forschungsgemeinschaft, the Alexander-von-Humboldt-Stiftung, and the Russian Foundation for Basic Research for financial support. Useful discussions with A. V. Goltsev and V. V. Pavlov are appreciated.

*Electronic address: fiebig@janeway.physik.uni-dortmund.de

[1] *Numerical Data and Functional Relationships*, Landolt-Börnstein, New Series, Group III, Vol. 16a (Springer-Verlag, Berlin, 1981).

[2] E.F. Bertaut and M. Mercier, Phys. Lett. **5**, 27 (1963).

[3] W. C. Koehler, H. L. Yakel, E. O. Wollan, and J. W. Cable, *Proceedings of the 4th Conference on Rare-Earth Research* (Gordon and Breach, New York, 1965), pp. 63–75; Phys. Lett. **9**, 93 (1964).

[4] M. Fiebig, C. Degenhardt, and R.V. Pisarev, Phys. Rev. Lett. **88**, 027203 (2002).

[5] M. Fiebig, D. Fröhlich, K. Kohn, St. Leute, Th. Lottermoser, V.V. Pavlov, and R.V. Pisarev, Phys. Rev. Lett. **84**, 5620 (2000).

[6] M. Fiebig, D. Fröhlich, K. Kohn, and Th. Lottermoser, Appl. Phys. Lett. **77**, 4401 (2000).

[7] M. Fiebig, D. Fröhlich, S. Leute, and R.V. Pisarev, J. Appl. Phys. **83**, 6560 (1998).

[8] D.G. Tomuta, S. Ramakrishnan, G.J. Nieuwenhuys, and J.A. Mydosh, J. Phys.: Condens. Matter **13**, 4543 (2001).

[9] T. Iizuka-Sakano, E. Hanamura, and Y. Tanabe, J. Phys.: Condens. Matter **13**, 3031 (2001).

[10] G.A. Smolenskii and I.E. Chupis, Sov. Phys. Usp. **25**, 475 (1982).

[11] H. Schmid, Ferroelectrics **162**, 317 (1994).

[12] Antiferromagnetic interplane coupling of Mn^{3+} spins corresponds to the so-called parallel orientation of neighboring spins in Ref. 5. However, the present terminology is physically more reasonable since the upper and lower halfs of the unit cell are connected to each other via the operation $\underline{6}(0,0,c/2)$ (a 60° rotation in combination with a translation by $c/2$ along z and time reversal), where the time-reversal operation indicates the antiferromagnetic coupling between corresponding Mn^{3+} spins.

[13] *International Tables for X-ray Crystallography, Vol. A: Space-Group Symmetry*, edited by T. Hahn (Reidel, Boston, 1987).

[14] J.E. Greedan, M. Bieringer, J.F. Britten, D.M. Giaquinta, and H.C. zur Loye, J. Solid State Chem. **116**, 118 (1995).

[15] Z.J. Huang, Y. Cao, Y.Y. Sun, Y.Y. Xue, and C.W. Chu, Phys. Rev. B **56**, 2623 (1997).

[16] T. Katsufuji, S. Mori, M. Masaki, Y. Moritomo, N. Yamamoto, and H. Takagi, Phys. Rev. B **64**, 104419 (2001).

[17] H.W. Xu, J. Iwasaki, T. Shimizu, H. Sato, and N. Kamegashira, J.

Alloys Compd. **221**, 274 (1995).
[18] M. Bieringer and J.E. Greedan, J. Solid State Chem. **143**, 132 (1999).
[19] A. Muñoz, J.A. Alonso, M.J. Martínez-Lope, M.T. Casáis, J.L. Martínez, and M.T. Fernándes-Díaz, Phys. Rev. B **62**, 9498 (2000).
[20] B. Wanklyn, J. Mater. Sci. **7**, 813 (1972).
[21] C. Degenhardt, M. Fiebig, D. Fröhlich, T. Lottermoser, and R.V. Pisarev, Appl. Phys. B: Lasers Opt. **73**, 139 (2001).
[22] V.F. Kovalenko and E.L. Nagaev, Sov. Phys. Usp. **29**, 297 (1986).
[23] E.L. Nagaev, Pis'ma Zh. Eksp. Teor. Fiz. **6**, 484 (1967).
[24] V.F. Kovalenko, P.S. Kuts, and V.P. Sokhatskii, Sov. Phys. Solid State **24**, 80 (1982); V.F. Kovalenko, E.S. Kolezhuk, and P.S. Kuts, Sov. Phys. JETP **54**, 742 (1981).
[25] M. Fiebig, T. Satoh, K. Miyano, Y. Tomioka, and Y. Tokura, Phys. Rev. B **60**, 7944 (1999).
[26] V. Kiryukhin, D. Casa, J.P. Hill, B. Keimer, A. Vigliante, Y. Tomioka, and Y. Tokura, Nature (London) **386**, 813 (1997).
[27] G.M. Genkin, Y.N. Nozdrin, I.D. Tokman, and V.N. Shastin, JETP Lett. **35**, 199 (1982); G.M. Genkin, Y.N. Nozdrin, P.S. Rasenstein, and V.N. Shastin, Sov. Phys. Solid State **25**, 2135 (1983).
[28] E.L. Nagaev, Sov. Phys. Solid State **27**, 1123 (1985).
[29] S. Kurita, K. Toyokawa, K. Tsushima, and S. Sugano, Solid State Commun. **38**, 235 (1981).
[30] M. Fiebig (unpublished).